

Comparative Analysis of Prediction Accuracy for Drifting Buoy Data Using CNN (Conv1D) and GRU Deep Learning Models with Varying Data Volumes

Trong, N. G.,^{1,2} Thanh, P. T.,^{3*} Quang, P. N.,^{1,2} Tinh, L. D.,¹ Manh, V. D.,⁴ Vinh, T. D.⁵ and Elshewy, M. A.⁶

¹Hanoi University of Mining and Geology, Hanoi, Vietnam

E-mail: nguyengiatrong@humg.edu.vn, phamngocquang@humg.edu.vn, leductinh@humg.edu.vn

²Geodesy and Environment Research Group, Hanoi University of Mining and Geology, Hanoi, Vietnam

³Vietnam National University of Forestry, E-mail: trungthanhphung@gmail.com

⁴Hanoi University of Natural Resources and Environment, Hanoi, Vietnam, E-mail: Vdmanh@hunre.edu.vn

⁵Viet Nam's People Naval Hydrographic and Oceanographic Department, Vietnam

E-mail: vinhhtduc@gmail.com

⁶Department of Civil Engineering, Faculty of Engineering, Al-Azhar University, Cairo, Egypt

E-mail: MohamadElshewy.2214@azhar.edu.eg

*Corresponding Author

DOI: <https://doi.org/10.52939/ijg.v21i4.4073>

Abstract

Drifting buoy data plays a vital role in climate and oceanographic research, offering critical insights into ocean surface dynamics, currents, and weather patterns. Accurate trajectory prediction of drifting buoys improves maritime weather forecasting, supports climate change research, and aids in search and rescue operations at sea. This research explores the application of two deep learning models, CNN (Conv1D) and GRU (1D), to predict buoy trajectories. The study utilizes the timestamped geographical coordinate datasets, which were processed and divided into training and testing sets. Both models were optimized using the Adam algorithm and Huber loss function, with hidden layer filter configurations of 64, 128, and 256. Model performance was evaluated using MSE, RMSE, MAE, R², Cohen's Kappa, and F1-score. Results indicate that CNN (Conv1D) consistently outperforms GRU, particularly with 256 filters, achieving significantly lower RMSE and MAE values, demonstrating higher predictive accuracy. While GRU exhibited performance fluctuations across different filter configurations, CNN (Conv1D) maintained stable accuracy across varying dataset conditions. Notably, CNN (Conv1D) achieved at least 50% greater accuracy than GRU while preserving a near-perfect correlation to input data. The study highlights the critical role of high-resolution data in enhancing prediction reliability, as lower-resolution or highly variable datasets negatively impact model performance. Additionally, it underscores the importance of effective preprocessing techniques for handling missing data to ensure robust predictions. This research advances deep learning applications in marine studies by optimizing trajectory forecasting models. Future work should explore hybrid approaches integrating Conv1D with other architectures or leveraging transformer models to enhance long-term prediction accuracy. These findings provide a reliable framework for oceanographic research, maritime navigation, and environmental monitoring in dynamic marine conditions.

Keywords: CNN (Conv1D), Deep Learning Models, Drifting Buoy Data, GRU, Time-series Prediction

1. Introduction

Numerous studies highlight the significance of drifting buoy data in various applications. For instance, the impact of station density on Numerical Weather Prediction (NWP) in the North Atlantic has been explored, demonstrating that halving station density disproportionately reduces forecast effectiveness [1].

This underscores the importance of dense station networks, especially in regions with strong atmospheric activity. However, the lack of pressure sensors at nearly half of the drifting buoy stations poses challenges, prompting recommendations to improve pressure data collection in critical regions like the Arctic and the Gulf Stream.

Similarly, the importance of pressure data from drifting buoys has been analyzed through observational system experiments [2]. Denial experiments revealed that excluding pressure data significantly increases forecast errors for pressure, temperature, and wind fields globally, underscoring the buoys' critical role in the World Meteorological Organization's global observation network.

Innovative technologies for drifting buoy applications are also being developed. Recent advancements include a rescue buoy network utilizing AIS and Beidou systems for search-and-rescue operations [3]. The need for precise short-term drift simulations, particularly in hydrological emergencies like oil spills, has been emphasized, highlighting the necessity of coupling atmospheric and oceanic models [4]. The evaluation of four ocean drift forecasting models using extensive drifting buoy data in Canada's St. Lawrence Bay has shown that incorporating Stokes drift into models reduces trajectory prediction errors by 34 - 40%, with the best results achieved through combined models integrating near-surface corrections and Stokes drift [5]. Studies have also analyzed the FOAM system's near-surface current predictions using drifting buoy trajectories, identifying biases in the Southern Ocean due to missing buoy bottoms [6]. Hyper-ensemble techniques applied to buoy drift forecasting have revealed that dynamic methods reduce forecast errors by at least threefold compared to individual models [7].

Advancements in deep learning methods have also enhanced trajectory prediction. For instance, DriftNet, a deep learning framework for simulating Lagrangian drift, has excelled in surface drift modeling [8]. The validation of OpenDrift, an open-source Lagrangian particle trajectory modeling system for oil spill simulations, demonstrated improved accuracy through factors like Stokes drift and currents [9]. Machine learning techniques further enhance model precision. The combination of regression neural networks with drifting buoy and satellite data has optimized surface current predictions in the Gulf of Mexico, achieving improved spatial and temporal resolution [10]. Additionally, acoustic depth measurement buoys have been utilized to improve tropical tuna fishing efficiency, achieving detection accuracies of 75 - 85% [11]. Statistical methods like linear regression and support vector machines have also demonstrated success in predicting water current velocity [12].

Global Navigation Satellite System (GNSS)-based studies have contributed to water level and

wave movement measurements. Compact GNSS-equipped buoys have been developed for measuring river water levels with mean errors below 2 cm [13]. Free Ocean Wave Data (FOWD) has been introduced for analyzing extreme wave activity, enabling accurate wave height predictions [14]. Machine learning approaches, such as the Extra Trees (ET) algorithm, have further improved wave height predictions with greater accuracy [15]. High-frequency monitoring systems combined with machine learning have enabled innovative solutions like soft sensors for chlorophyll-a (Chl-a) data, offering rapid and cost-effective water monitoring [16]. Cognitive sensor frameworks with deep learning have been introduced for real-time drifting object prediction, demonstrating the effects of wind and currents on drift coefficients [17]. Additionally, the CNN-BiGRU-Attention model has shown excellent generalization and convergence for long-term trajectory predictions under varying marine conditions [18].

The analysis of drifting buoy data plays a crucial role in predicting the trajectories of floating objects, ships, and oil spills, supporting maritime safety, search and rescue, and environmental incident response. Current models rely on weather, wave, and ocean forecast data but still have limitations, particularly in integrating drift factors. Therefore, this study focuses on improving the accuracy of buoy trajectory prediction, optimizing rescue operations, and minimizing maritime damage [19] and [20]. The CNN (Conv1D) and GRU models have demonstrated superior performance in geospatial data analysis, including spatial prediction of fluvial floods [21], groundwater data analysis [22], and intelligent network traffic prediction [23]. However, no studies have yet explored the application of these models in analyzing drifting buoy data at sea.

This study employs GRU and CNN (Conv1D) models to analyze time-series and spatial data. Using data from two drifting buoys, it evaluates the performance of these models with varying data volumes to understand their predictive accuracy and optimize their application in ocean studies. Convolutional Neural Networks (CNNs), particularly 1D CNNs (Conv1D), provide significant advantages in spatiotemporal data analysis. They effectively capture local spatial dependencies and reduce computational complexity through parallel processing, making them scalable for large datasets [24]. In contrast, GRUs excel in capturing long-term temporal dependencies but face inefficiencies due to their sequential processing nature [25].

2. Data and Methodology

2.1 Data Utilized

In the East Sea of Vietnam, a large amount of data from various drifting buoys is available [26]. From the collected dataset, the data from two drifting buoys, 49676 and 56644, were randomly selected as the experimental data for this study. Each dataset includes detailed information such as buoy ID, timestamp, geographical coordinates (latitude and longitude), and other environmental parameters (sea surface temperature), the flow velocity (represented by the speed of the drifting buoy) recorded at each location and time point, such as flow velocity and salinity [12].

Table 1 summarizes the key attributes of the experimental data. In Table 1, the time interval is set to 1 hour because the drifting buoy is programmed to record a dataset every hour. The datasets represent distinct time spans of observation to evaluate the prediction accuracy of deep learning models under varying data availability conditions. The geographic study area, delineated by a red boundary in Figure 1, is situated in the East Sea, part of the western Pacific Ocean. The East Sea exhibits a tropical monsoon climate with pronounced seasonal variations shaped by monsoon systems and oceanic circulation patterns.

Table 1: Information about the experimental data

| Description of Parameters | Drifting Buoy 56644 | Drifting Buoy 49676 |
|---------------------------|----------------------|----------------------|
| Start time | 20/11/2005 | 20/11/2004 |
| Stop time | 30/11/2005 | 13/12/2005 |
| Latitude (Min, Max) | 20.60624, 22.42329 | 14.29034, 22.92967 |
| Longitude (Min, Max) | 118.68426, 119.99723 | 107.95411, 119.99973 |
| Data sampling interval | 1 hour | 1 hour |

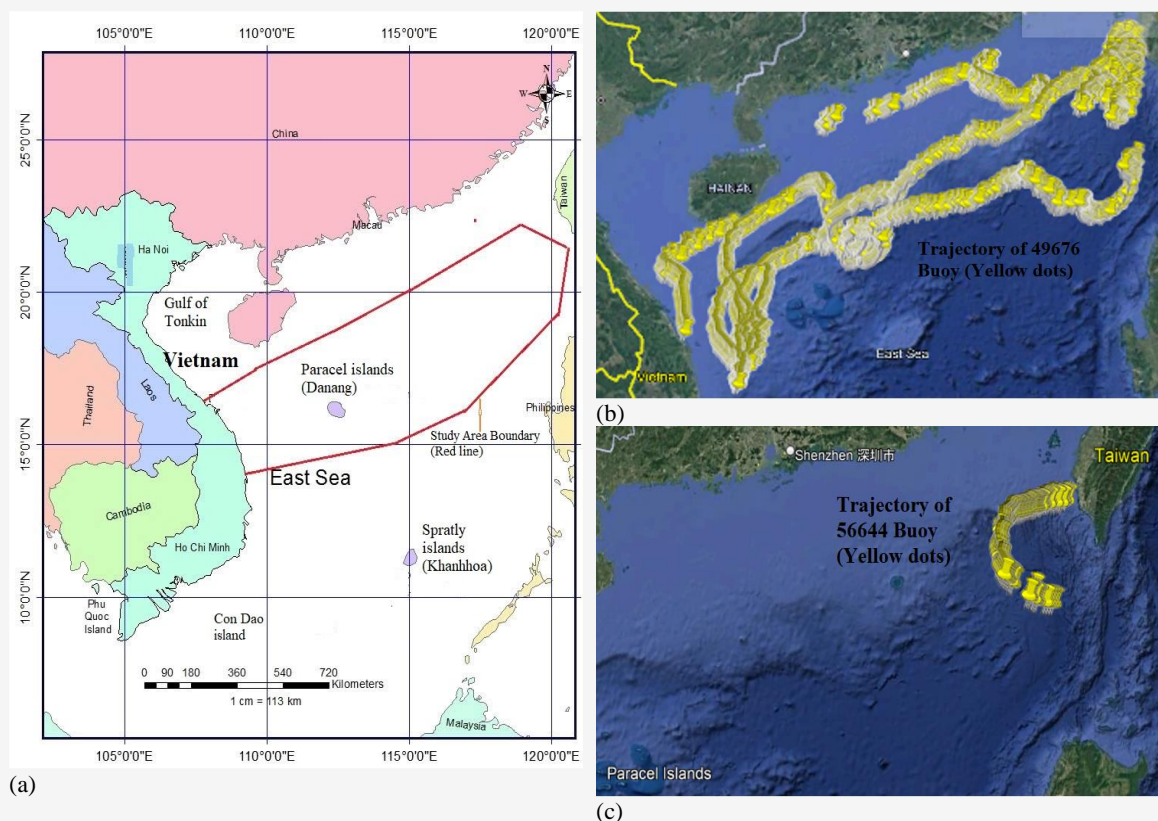


Figure 1: Study area: (a) Boundary of the study area (red line); (b) Trajectory of 49676 Buoy (yellow dots); and (c) Trajectory of 56644 Buoy (yellow dots)

It experiences two primary seasons: the rainy season, driven by the southwest monsoon (May - September), and the dry season, influenced by the northeast monsoon (October - April).

- *Rainy Season (May - September)*: Characterized by high temperatures exceeding 30°C and significant humidity due to warm, moist air from the Indian Ocean. Precipitation is abundant, particularly in central and southern regions, with annual rainfall often surpassing 2000 mm.
- *Dry Season (October - April)*: Marked by cooler, drier airflows from the Asian continent. Temperatures range between 20°C and 28°C, with reduced precipitation and calmer weather.

Additionally, the region is susceptible to typhoons, mainly between July and November, peaking from August to October. These events bring heavy rainfall, strong winds, and storm surges, impacting both marine and coastal ecosystems. Oceanic currents, such as the warm Kuroshio Current, significantly influence the sea's surface temperature and climate patterns, contributing to the region's dynamic environmental conditions [27].

2.2 Methodology

The initial datasets were processed to generate a structured input dataset containing parameters such as timestamp, latitude, and longitude for each buoy. These datasets were then partitioned into training and testing subsets to facilitate model evaluation. The experimental workflow is illustrated in Figure 2.

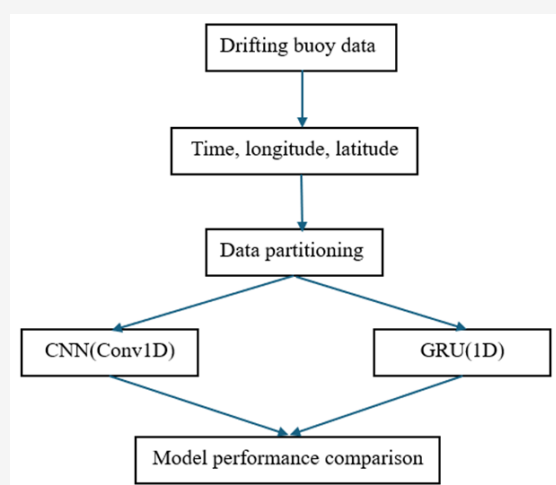


Figure 2: Experimental calculation process of the paper

The analyzed data were subjected to machine learning techniques, specifically CNN (Conv1D) and GRU (1D) models, selected for their efficacy in time series data processing [28][29] and [30]. The implementation utilized Python programming, leveraging TensorFlow and Scikit-learn libraries for model development and performance evaluation [31] and [32]. Key steps in the methodology include:

1. *Model Construction*: Models were configured with the Adam optimization algorithm, the Huber loss function, and varying numbers of filters in hidden layers (64, 128, and 256).
2. *Performance Metrics*: Model evaluation was based on metrics such as Mean Squared Error (MSE), Root Mean Squared Error (RMSE), Mean Absolute Error (MAE), Cohen's Kappa, R², and F1-Score [33].

The final outcomes of the analysis included graphical representations of model performance saved in a Word file, alongside .csv files containing actual and predicted values for training and testing datasets. To prepare the input dataset for the CNN (Conv1D) and GRU models, the raw buoy data in .xlsx format was preprocessed. This dataset contained multiple columns, including ID, time, latitude, longitude, sea surface temperature, buoy velocity in the north and east directions, and buoy characteristics. Using a Python-based data processing program, the .xlsx file was converted into a .csv format for further analysis. Unnecessary attributes were removed, retaining only essential features: time, latitude, and longitude. This preprocessing step ensured a clean and structured dataset, facilitating effective model training. Additionally, missing values were handled appropriately, and the data was formatted for compatibility with deep learning algorithms. This refined dataset was then used as input for predicting buoy drift trajectories.

During the model development process, the dataset was split into a training set and a testing set with a ratio of 70% and 30%, respectively. The outlier detection process was not addressed in this study. The computer program was developed using the latest versions of library functions and executed on a Dell 7520 workstation. The performance comparison of the CNN (Conv1D) model and the GRU model, as described in Figure 2, is conducted by comparing the magnitudes of performance metrics such as MAE, MSE, RMSE, R-squared, F1-score, and Kappa.

2.3 CNN(Conv1D) and GRU Model

2.3.1 CNN(Conv1D) model

A 1D Convolutional Neural Network (CNN) is a deep learning architecture designed to process sequential data, such as time series and spatiotemporal datasets. Unlike 2D CNNs that operate on images, 1D CNNs apply convolutional filters along a single temporal or spatial dimension, enabling efficient feature extraction from sequential patterns [34]. The fundamental operation in a 1D CNN is the convolution, mathematically expressed in equation 1.

$$y_i = \sum_{j=0}^{k-1} x_{i+j} w_j + b$$

Equation 1

Where:

- y_i is the output feature at position i ;
- x_{i+j} is the input sequence;
- w_j is the convolutional filter (kernel) of size k ;
- b is the bias term.

A Conv1D model typically consists of multiple layers, each playing a distinct role in processing sequential data:

1. Convolutional Layer: Applies multiple filters to extract meaningful local patterns.
2. Activation Function: Introduces non-linearity, commonly using the ReLU function as defined in equation 2.

$$F(x) = \max(0, x)$$

Equation 2

3. Pooling Layer: Reduces the dimensionality of feature maps via max-pooling defined in equation 3.

$$y_i = \max(x_{i:i+k})$$

Equation 3

4. Fully Connected Layer: Integrates extracted features for final prediction. The CNN (Conv1D) model used in this study is constructed as described in Figure 3.

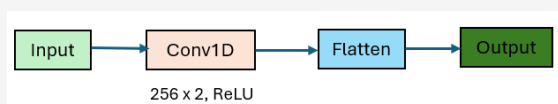


Figure 3: Flowchart illustrating the structure of the CNN (Conv1D) model

2.3.2 GRU model

Gated Recurrent Unit (GRU) is a type of recurrent neural network (RNN) designed to handle sequential data effectively by addressing the vanishing gradient problem. Introduced by [35], GRU is a simplified variant of Long Short-Term Memory (LSTM) networks but with fewer parameters, making it computationally efficient while maintaining strong performance in sequence modeling tasks. A GRU unit consists of two primary gates: the reset gate and the update gate. These gates regulate how much past information is retained and how much new information is incorporated. The mathematical representation of these gates is defined in equations 4 and 5.

$$z_i = \sigma(W_z x_i + U_z h_{i-1} + b_z)$$

Equation 4

$$r_i = \sigma(W_r x_i + U_r h_{i-1} + b_r)$$

Equation 5

Where:

- z_i is the update gate that controls the degree to which the previous hidden state is retained
- r_i is the reset gate that determines how much past information is forgotten
- b is bias
- σ is the sigmoid activation function.
- W and U are weight matrices

The candidate hidden state (\tilde{h}_i) is computed from equation 6.

$$\tilde{h}_i = \tanh(W_h x_i + U_h (r_i h_{i-1}) + b_h)$$

Equation 6

Finally, the hidden state h_i at time step t is updated in equation 7.

$$h_i = h_{i-1}(1 - z_i) + z_i \tilde{h}_i$$

Equation 7

This formulation allows GRU to adaptively retain long-term dependencies without excessive memory usage. Due to its gating mechanism, GRU can efficiently capture complex temporal relationships while remaining less computationally demanding than LSTM. The GRU model used in this study is constructed as described in Figure 4.

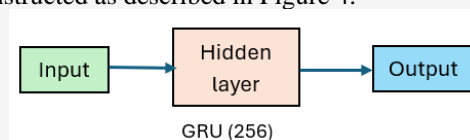


Figure 4: Structure of the GRU model

2.3.3 Model accuracy evaluation

Mean Squared Error (MSE): MSE measures the average squared difference between predicted (\hat{y}_i) and actual (y_i) values. It penalizes larger errors more than smaller ones: The MSE is determined from equation 8.

$$MSE = \frac{1}{n} \sum_{i=1}^n (y_i - \hat{y}_i)^2$$

Equation 8

Where n is the number of observations. A lower MSE indicates better model performance [36].

Root Mean Squared Error (RMSE): RMSE is the square root of MSE, which retains the same unit as the predicted variable, making it more interpretable: It is determined from equation 9.

$$RMSE = \sqrt{\frac{1}{n} \sum_{i=1}^n (y_i - \hat{y}_i)^2}$$

Equation 9

Mean Absolute Error (MAE): MAE calculates the mean absolute differences between actual and predicted values as defined in equation 10.

$$MAE = \frac{1}{n} \sum_{i=1}^n |y_i - \hat{y}_i|$$

Equation 10

Unlike MSE, it does not penalize large errors as strongly, making it more robust to outliers [37].

Coefficient of Determination (R^2): R^2 measures how well the model explains variance in the target variable. R^2 is defined in equation 11.

$$R^2 = 1 - \frac{\sum (y_i - \hat{y}_i)^2}{\sum (y_i - \bar{y})^2}$$

Equation 11

Where \bar{y} is the mean of actual values. An R^2 close to 1 suggests a strong predictive capability [38].

F1-score: F1-score evaluates classification models by combining precision and recall as defines in equation 12.

$$F1 - score = 2 \frac{Precision \times Recall}{Precision + Recall}$$

Equation 12

Cohen's Kappa (k): Cohen's Kappa assesses inter-rater agreement while adjusting for chance [21]. It can be determined from equation 13.

$$k = \frac{P_o - P_e}{1 - P_e}$$

Equation 13

Where P_o is observed agreement, and P_e is expected agreement under randomness.

The Adam optimizer was chosen for its efficiency in handling sparse gradients and its adaptive learning rate, which enhances convergence speed and stability by combining the benefits of momentum-based SGD and RMSProp. The Huber loss function was selected as it balances mean squared error (MSE) and mean absolute error (MAE), making the model more robust to outliers while maintaining sensitivity to small errors, which is particularly useful for sequential data with occasional large deviations. During training, the learning rate is automatically adapted by Adam, while a batch size of 16 was used to ensure a balance between computational efficiency and gradient stability. The model was trained for 200 epochs, providing sufficient learning while mitigating the risk of overfitting.

3. Results and Discussion

This section presents a detailed analysis of the performance of GRU and CNN (Conv1D) models in predicting the trajectories of drifting buoys. The results are discussed with reference to datasets from buoys 56644 and 49676, comparing the accuracy and robustness of the models across different configurations of the hidden layer filters.

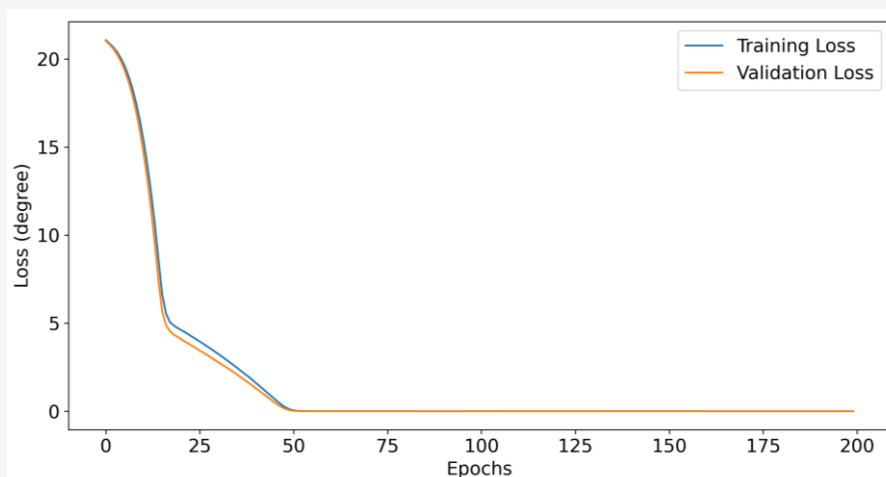
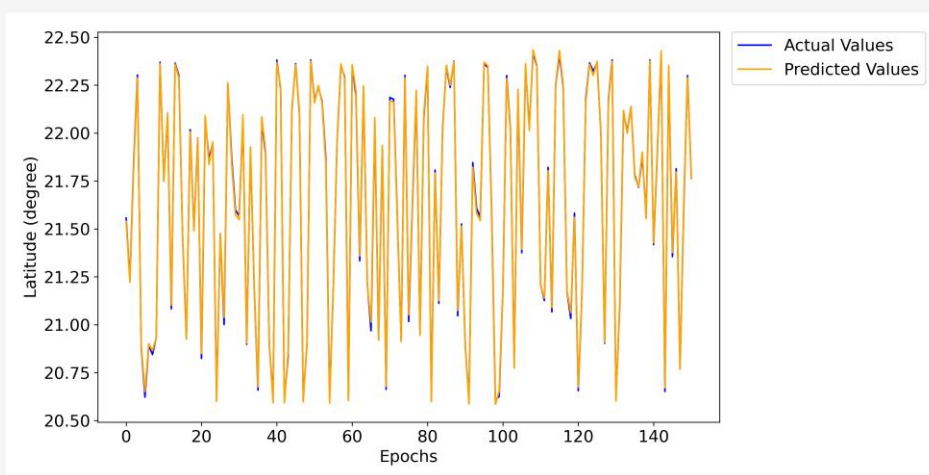
3.1 Analysis Results for Drifting Buoy Dataset 56644

3.1.1 GRU model performance

The results of analyzing buoy dataset 56644 using the GRU model are summarized in Table 2. The data clearly indicate that increasing the number of filters in the hidden layer enhances model performance. Specifically, as the number of filters increased from 64 to 256, the mean squared error (MSE) reduced from 0.000587 to 0.000227. Correspondingly, the root mean square error (RMSE) and mean absolute error (MAE) decreased, indicating improved predictive accuracy. Additionally, the R-squared (R^2) values, ranging from 99.81% to 99.92%, underscore the high degree of model fit to the dataset.

Table 2: Results of analyzing the 56644-buoy data with the GRU(1D) model

| Number of filters | MSE (Degree) | RMSE (Degree) | MAE (Degree) | R ² | k | F1-Score |
|-------------------|------------------------|-------------------------|-------------------------|----------------|-----|----------|
| 64 | 0.587×10^{-3} | 24.224×10^{-3} | 20.047×10^{-3} | 0.998 | 1.0 | 1.0 |
| 128 | 0.428×10^{-3} | 20.692×10^{-3} | 18.065×10^{-3} | 0.999 | 1.0 | 1.0 |
| 256 | 0.227×10^{-3} | 15.072×10^{-3} | 12.813×10^{-3} | 0.999 | 1.0 | 1.0 |

**Figure 5:** Loss function values for drifting buoy data 56644 using GRU with 256 filters**Figure 6:** Predicted vs. actual values for the training dataset of buoy 56644 using GRU with 256 filters

The visualizations in Figures 5 to 7 further validate these findings. Figure 5 demonstrates the steady decline in the loss function during training, while Figures 6 and 7 illustrate the close alignment between the predicted and actual values for both training and test datasets when using 256 filters in the hidden layer.

3.1.2 CNN (Conv1D) model performance

The CNN (Conv1D) model results are shown in Table 3. Unlike the GRU model, the CNN's performance did not follow a strictly linear improvement pattern as the number of filters

increased. However, the highest performance was achieved with 256 filters, yielding an MSE of 0.000093, RMSE of 0.009630, and MAE of 0.007697. These values represent a significant improvement over the GRU model, with RMSE and MAE reductions of nearly 50%. The graphical representations in Figures 8 to 10 further highlight the CNN's superior predictive capabilities. Figure 8 shows the loss function's rapid convergence, while Figures 9 and 10 demonstrate near-perfect alignment between actual and predicted values in the training and test datasets.

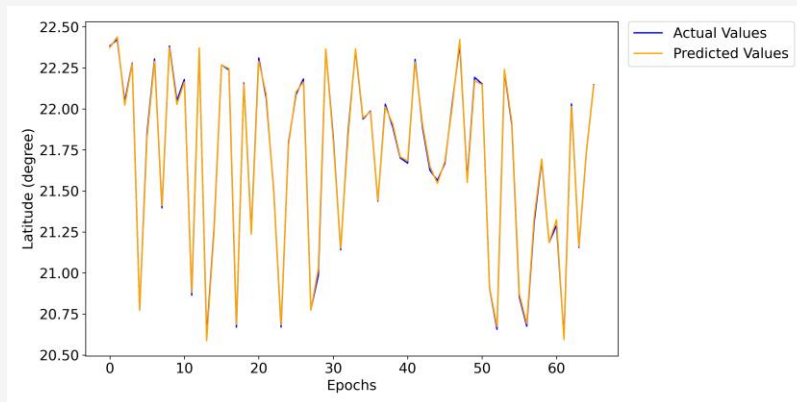


Figure 7: Predicted vs. actual values for the test dataset of buoy 56644 using GRU with 256 filters

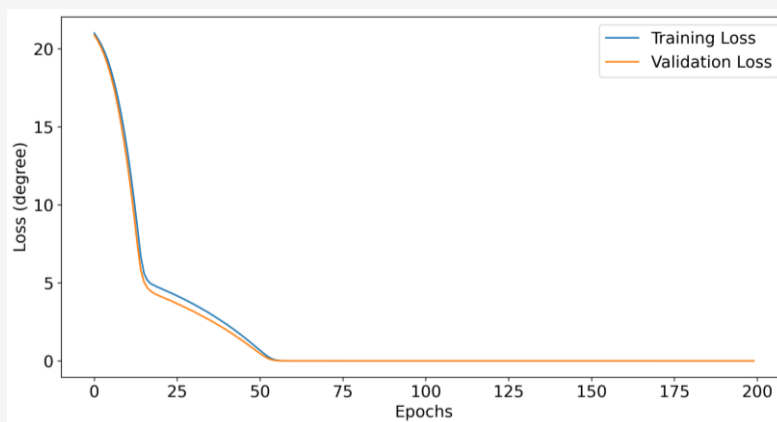


Figure 8: Loss function values for drifting buoy data 56644 using CNN(Conv1D) with 256 filters

Table 3: Results of analyzing the 56644-buoy data with the CNN(Conv1D) model

| Number of filters | MSE (Degree) | RMSE (Degree) | MAE (Degree) | R ² | k | F1-Score |
|-------------------|------------------------|-------------------------|-------------------------|----------------|-----|----------|
| 64 | 0.472×10^{-3} | 21.733×10^{-3} | 17.747×10^{-3} | 0.999 | 1.0 | 1.0 |
| 128 | 1.500×10^{-3} | 38.721×10^{-3} | 31.736×10^{-3} | 0.995 | 1.0 | 1.0 |
| 256 | 0.093×10^{-3} | 9.630×10^{-3} | 7.697×10^{-3} | 1.000 | 1.0 | 1.0 |

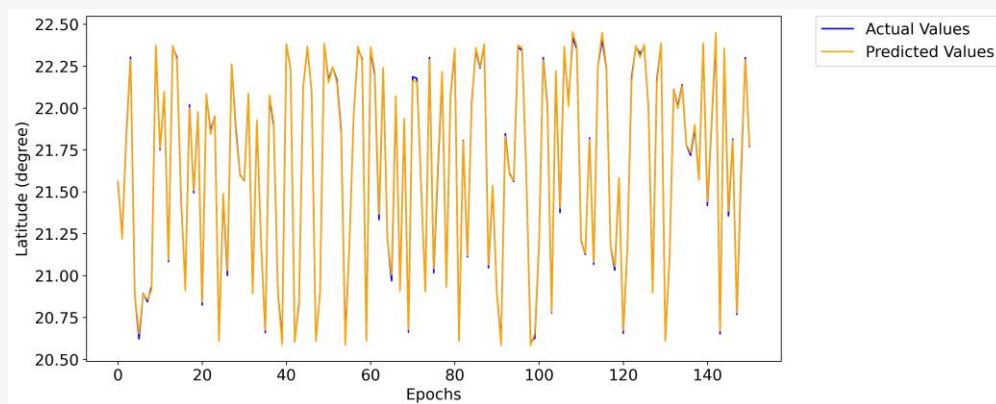


Figure 9: Predicted vs. actual values for the training dataset of buoy 56644 using CNN(Conv1D) with 256 filters

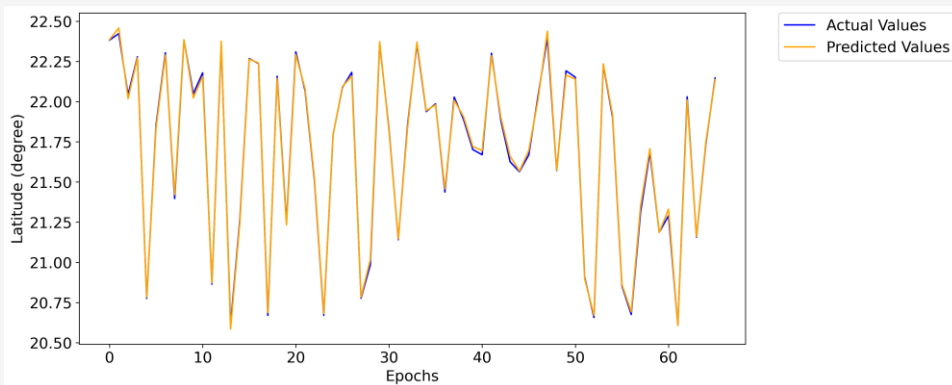


Figure 10: Predicted vs. actual values for the test dataset of buoy 56644 using CNN(Conv1D) with 256 filters

The analysis results highlight key differences in the performance of GRU and CNN (Conv1D) models when applied to buoy dataset 56644. While both models achieved high levels of accuracy, CNN (Conv1D) consistently outperformed GRU, achieving superior prediction precision and lower error metrics. The reduction in RMSE and MAE values for CNN (Conv1D) underscores its robustness in capturing the spatiotemporal dynamics of drifting buoy data. These findings validate that CNN (Conv1D) is better suited for time-series data analysis in oceanographic applications. Moreover, the study underscores the importance of optimizing model configurations, such as the number of filters, to achieve maximal performance in predictive tasks.

The performance comparison between GRU and CNN (Conv1D) across different filter configurations reveals significant variations in their predictive accuracy. As the number of filters increases, the CNN (Conv1D) model demonstrates a more stable reduction in error metrics, with MSE, RMSE, and MAE consistently decreasing, indicating enhanced learning capability. In contrast, the GRU model exhibits fluctuations in performance, particularly at 128 filters, where a notable increase in error values is observed before improving at 256 filters. This suggests that GRU may be more sensitive to hyperparameter tuning and requires careful configuration to achieve optimal results. The differences in performance highlight the structural advantages of CNN (Conv1D) in extracting spatial dependencies more effectively than GRU, which relies on sequential processing. The consistently high R^2 values across both models indicate strong predictive reliability, yet CNN (Conv1D)'s lower error values suggest superior feature extraction from the buoy dataset. The near-identical Kappa and F1-score values (both at 1.0) confirm that both models classify drift patterns effectively, but CNN (Conv1D)

offers better numerical precision. Error pattern analysis further reinforces these observations. GRU's fluctuating RMSE and MAE values imply sensitivity to filter adjustments, potentially leading to inconsistent generalization. CNN (Conv1D), on the other hand, maintains a downward trend in error metrics, affirming its robustness in learning complex spatiotemporal relationships. These findings suggest that CNN (Conv1D) not only provides better predictive accuracy but also exhibits greater stability in handling varying filter configurations, making it a more reliable choice for buoy trajectory prediction.

3.2 Analysis Results for Drifting Buoy Dataset 49676

The performance of the GRU and CNN (Conv1D) models for predicting the trajectory of buoy dataset 49676 is detailed below. Changes in prediction accuracy are analyzed as the number of filters in the hidden layer varies between 64, 128, and 256 filters.

3.2.1 GRU model performance

The results of the GRU model for the 49676 datasets are summarized in Table 4. The model's prediction performance showed inconsistency with changes in the number of filters. Notably, the configuration with 128 filters achieved the highest accuracy, with an MSE of 6.51×10^{-7} , RMSE of 0.000807, and MAE of 0.000623. These metrics underscore the model's ability to provide highly precise predictions under optimal configurations. The data in Tables 2 and 4 show that when the input data volume is larger, the prediction accuracy with the GRU model is also higher. The graphs in Figures 11 through 13 further illustrate the GRU model's performance. Figure 11 shows the consistent reduction of the loss function, while Figures 12 and 13 demonstrate excellent agreement between predicted and actual values for both training and test datasets, particularly when using 128 filters.

Table 4: Analysis results of the 49676-buoy dataset with the GRU(1D) model

| Number of filters | MSE (Degree) | RMSE (Degree) | MAE (Degree) | R ² | k | F1-Score |
|-------------------|------------------------|-------------------------|-------------------------|----------------|-----|----------|
| 64 | 0.154×10^{-3} | 12.413×10^{-3} | 12.403×10^{-3} | 1.0 | 1.0 | 1.0 |
| 128 | 6.51×10^{-7} | 0.807×10^{-3} | 0.623×10^{-3} | 1.0 | 1.0 | 1.0 |
| 256 | 8.90×10^{-6} | 2.983×10^{-3} | 2.100×10^{-3} | 1.0 | 1.0 | 1.0 |

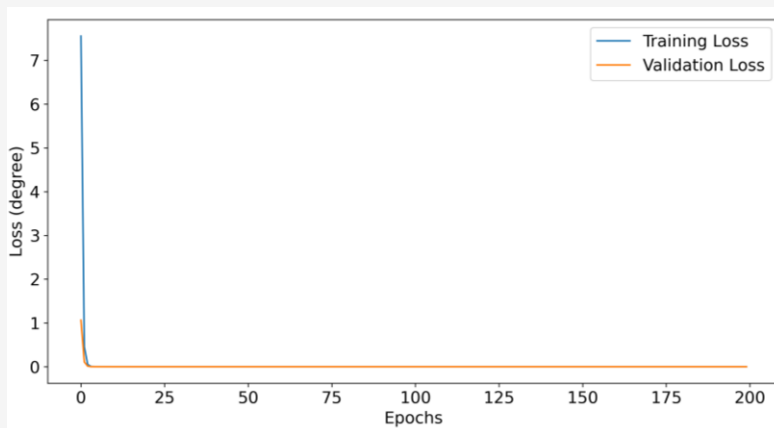
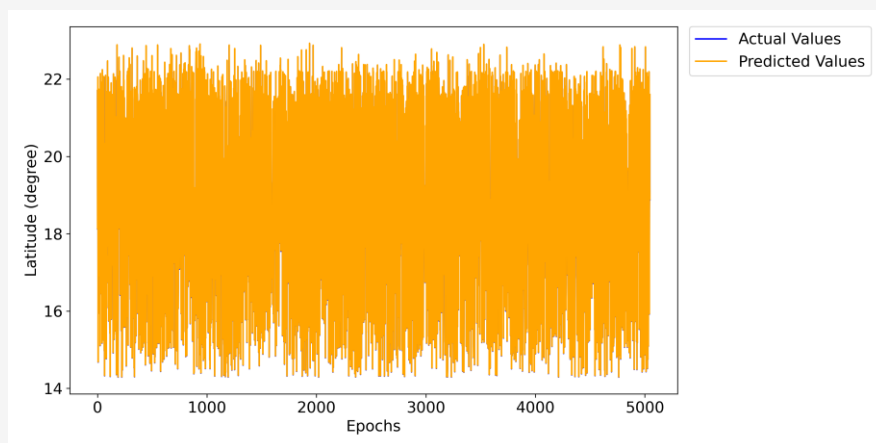
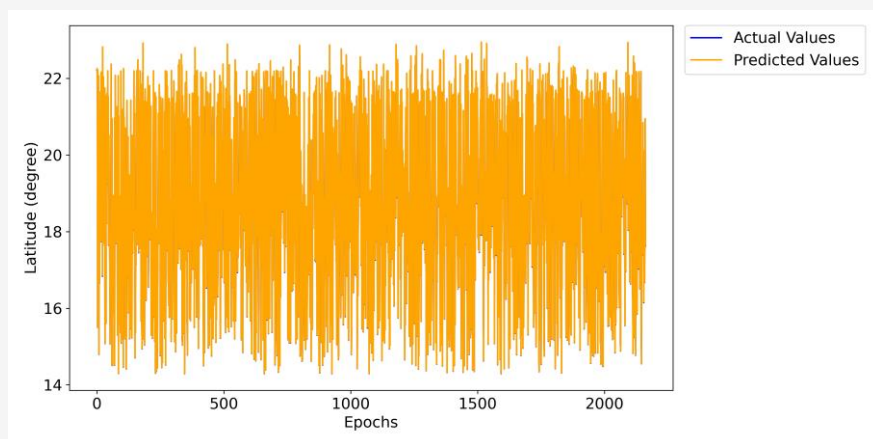
**Figure 11:** Loss function values for buoy 49676 using GRU with 128 filters**Figure 12:** Predicted vs. actual values for the training dataset of buoy 49676 using GRU with 128 filters**Figure 13:** Predicted vs. actual values for the test dataset of buoy 49676 using GRU with 128 filters

Table 5: Analysis results of the 49676-buoy dataset with the CNN(Conv1D) model

| Number of filters | MSE (Degree) | RMSE (Degree) | MAE (Degree) | R ² | k | F1-Score |
|-------------------|------------------------|------------------------|------------------------|----------------|-----|----------|
| 64 | 2.75×10^{-9} | 5.25×10^{-5} | 4.48×10^{-5} | 1.0 | 1.0 | 1.0 |
| 128 | 4.89×10^{-12} | 2.21×10^{-6} | 1.78×10^{-6} | 1.0 | 1.0 | 1.0 |
| 256 | 1.90×10^{-7} | 0.436×10^{-3} | 0.426×10^{-3} | 1.0 | 1.0 | 1.0 |

3.2.2 CNN (Conv1D) model performance

The results of the CNN (Conv1D) model are summarized in Table 5. The prediction accuracy was highest with 128 filters, yielding an MSE of 4.89×10^{-12} , RMSE of 2.21×10^{-6} , and MAE of 1.78×10^{-6} . These metrics represent exceptional precision and demonstrate the model's capability for handling this dataset effectively. Despite minor variations in performance as the number of filters changed, the degree of fit to the data was consistently 100%. From the data in Tables 2 to 5, it can be seen that the highest forecasting performance for both the GRU and CNN(Conv1D) models is achieved with the same number of filters in the hidden layer. Similar to the forecasting case using the GRU function, the degree of fit between the model and the input data is maximal, corresponding to a value of 100%.

The results indicate that while both GRU and CNN (Conv1D) achieve perfect model fit ($R^2 = 1.0$, $Kappa = 1.0$, $F1\text{-Score} = 1.0$) across all filter configurations, the detailed error metrics reveal nontrivial variations in predictive precision. Notably, for CNN (Conv1D), the lowest RMSE (2.21×10^{-6}) and MAE (1.78×10^{-6}) occur at 128 filters, demonstrating the model's peak accuracy at this configuration. However, performance slightly deteriorates at 256 filters, as reflected in increased RMSE (4.36×10^{-4}) and MAE (4.26×10^{-4}). This trend suggests that CNN (Conv1D) may reach an optimal capacity at a certain filter threshold, beyond which additional filters introduce redundancy or overfitting effects.

For the GRU model, performance fluctuations are more pronounced, particularly at 256 filters, where RMSE (2.983×10^{-3}) and MAE (2.100×10^{-3}) increase compared to 128 filters. This implies that, unlike CNN (Conv1D), GRU's sequential nature makes it more sensitive to filter count variations, potentially leading to unstable learning when the filter size is too large. These results suggest that CNN (Conv1D) benefits from an intermediate number of filters for optimal performance, whereas GRU requires a more refined tuning strategy to maintain predictive consistency. Additionally, the observed variations may stem from computational efficiency differences between the two models. While increasing filter size enhances feature extraction, excessive filters may

introduce unnecessary complexity, leading to slower convergence and optimization challenges. This is particularly relevant for CNN (Conv1D), where a well-balanced filter configuration is crucial to maintaining generalization while avoiding overfitting. These findings emphasize the importance of systematic hyperparameter tuning to achieve the best trade-off between accuracy and computational efficiency. The inconsistent improvements in CNN (Conv1D) performance with an increasing number of filters can be attributed to several factors. The data indicate improvements from 64 to 128 filters. However, performance deteriorates at 256 filters, as shown by the increase in MSE, RMSE, and MAE. One possible reason is overfitting, where the model captures noise instead of meaningful patterns when the number of filters is too high. This is particularly evident in the second dataset, where performance improves from 64 to 128 filters but degrades at 256 filters, as indicated by the increase in MSE, RMSE, and MAE. Additionally, increasing the number of filters may lead to diminishing returns due to redundant feature extraction, where additional filters do not contribute new information but rather amplify existing noise. Computational complexity also plays a role, as excessive filters may lead to optimization challenges, making training less stable. These variations suggest that an optimal number of filters exists for CNN (Conv1D), and blindly increasing them may not always yield better performance. Therefore, careful hyperparameter tuning and validation are necessary to determine the best configuration for a given dataset.

Figures 14 through 16 provide additional insights into the CNN (Conv1D) model's performance. Figure 14 highlights the smooth and rapid convergence of the loss function. Figures 15 and 16 depict near-perfect alignment between actual and predicted values for training and test datasets when using 128 filters. The results indicate that both the GRU and CNN (Conv1D) models achieve exceptional prediction accuracy for buoy 49676. Notably, both models achieved their best performance with 128 filters, highlighting the importance of tuning model configurations for optimal results.

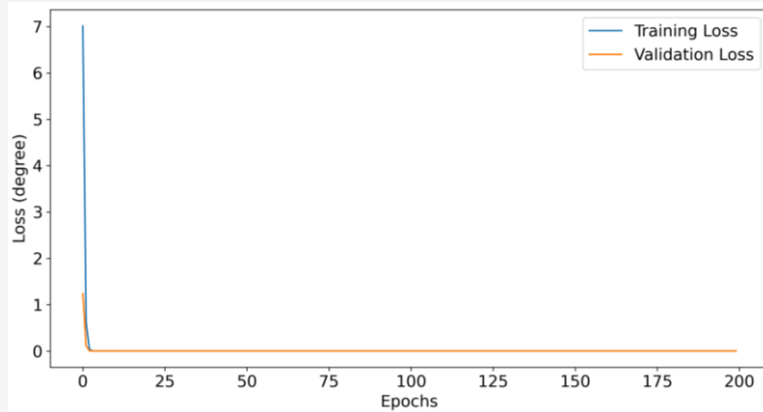


Figure 14: Loss function values for buoy 49676 using CNN (Conv1D) with 128 filters

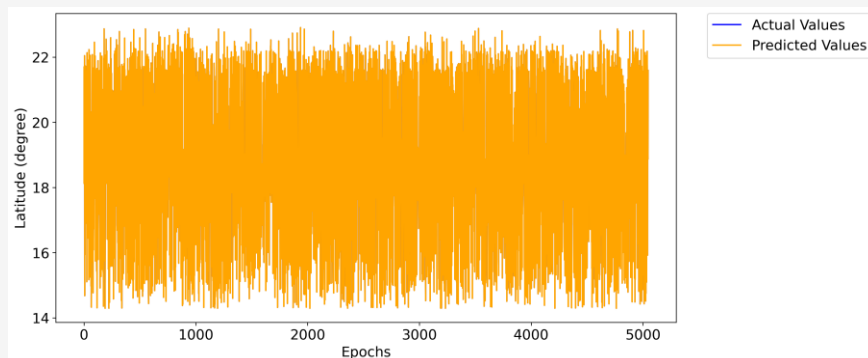


Figure 15: Predicted vs. actual values for the training dataset of buoy 49676 using CNN (Conv1D) with 128 filters

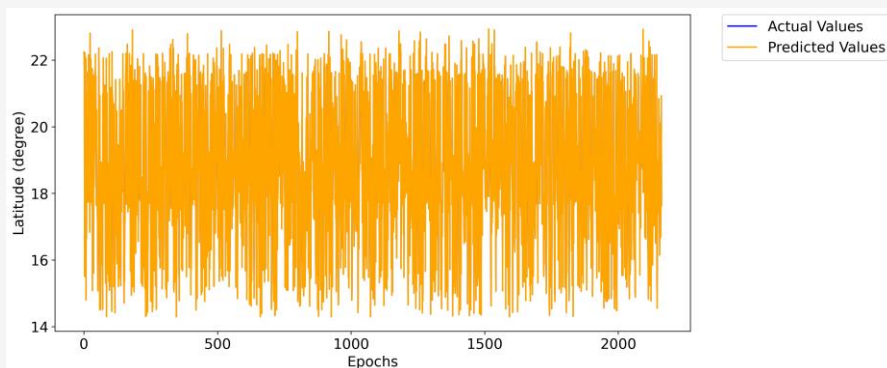


Figure 16: Predicted vs. actual values for the test dataset of buoy 49676 using CNN (Conv1D) with 128 filters

The CNN (Conv1D) model demonstrated marginally superior performance compared to GRU, particularly in terms of precision and stability. These findings reinforce the suitability of CNN (Conv1D) for time-series predictions in oceanographic studies, while also highlighting the potential of GRU models under certain configurations. The ability of both models to achieve near-perfect fits underscores their robustness in handling complex, spatiotemporal data such as drifting buoy trajectories.

3.3 Compare with Similar Studies

The results of this study align with previous research emphasizing the effectiveness of deep learning techniques in time-series prediction tasks. For instance, DriftNet, a deep learning framework developed for Lagrangian drift modeling, demonstrated high accuracy in predicting oceanic drift patterns by leveraging spatiotemporal data [8].

Table 6: Summary of comparative studies on deep learning models for trajectory prediction

| Studies | Method used | Key findings | Comparison to this study |
|--|--|---|---|
| DriftNet [8] | Deep learning framework for lagrangian drift | High accuracy in predicting oceanic drift patterns using spatiotemporal data | The present study shows similar accuracy using purely data-driven approaches (CNN and GRU) without physical models. |
| OpenDrift [9] | Open-source trajectory modeling system | Improved prediction accuracy through integration of Stokes drift and currents | This study achieves comparable accuracy without explicit incorporation of environmental factors. |
| Hyper-Ensemble techniques [7] | Ensemble models for buoy drift forecasting | Reduced forecast errors by at least threefold compared to individual models | CNN (Conv1D) demonstrated superior predictive accuracy as a standalone model. |
| Stokes drift integration [5] | Integration of Stokes drift into prediction models | Reduced trajectory prediction errors by 34–40% | CNN (Conv1D) achieved similar error reductions with optimized neural network configurations. |
| Geospatial studies (Flood prediction) [21] | CNN (Conv1D) | High predictive accuracy with CNN(Conv1D) for spatial dependencies | This study extends their application to marine datasets, revealing CNN (Conv1D) outperforms GRU in trajectory prediction. |
| Groundwater data analysis [22] | GRU and CNN (Conv1D) | GRU and CNN effectively captured long-term and local dependencies | Similar strengths observed, but CNN (Conv1D) provided more robust predictions for drifting buoy data. |
| CNN for spatiotemporal data [34] | CNN (Conv1D) | Demonstrated robust performance for time-series data processing through parallel processing | Consistent with findings in this study where CNN (Conv1D) outperformed GRU in predictive accuracy and stability. |

Similarly, OpenDrift, an open-source trajectory modeling system validated for oil spill simulations, showed improved prediction accuracy by incorporating factors like Stokes drift and currents [9]. These studies highlight the importance of advanced modeling techniques for capturing dynamic oceanic processes.

While DriftNet and OpenDrift primarily focus on enhancing prediction accuracy through environmental parameters and physical modeling, the present study demonstrates the capability of purely data-driven approaches such as CNN (Conv1D) and GRU to achieve comparable levels of accuracy without requiring extensive physical parameterizations. This distinction underscores the versatility of deep learning methods in handling diverse datasets and prediction scenarios. In comparison to studies evaluating hyper-ensemble techniques for buoy drift forecasting, which achieved a threefold reduction in forecast errors [7], the results of the current study illustrate the potential for standalone models like CNN (Conv1D) to outperform ensemble approaches. The findings further align with research on the integration of Stokes drift into ocean drift models, which reduced trajectory prediction errors by up to 40% [5]. The present study complements this body of work by demonstrating that optimizing neural network architectures can yield similar error reductions, particularly when using high-resolution datasets. Moreover, studies on CNN and GRU applications in geospatial domains, such as flood prediction [21] and groundwater analysis [22], have reported high predictive accuracy, with GRU excelling in capturing

long-term temporal dependencies and CNN proving effective for spatial feature extraction. The current study builds upon these findings by applying CNN (Conv1D) and GRU to marine datasets, revealing that CNN (Conv1D) consistently outperforms GRU in trajectory prediction tasks, particularly when larger datasets are utilized. The observed limitations of GRU in handling large filter configurations, as indicated by performance fluctuations, corroborate findings in other studies where recurrent models exhibited sensitivity to hyperparameter tuning [35]. In contrast, CNN (Conv1D) demonstrated robust and stable performance, consistent with its reported strengths in handling spatiotemporal data through parallel processing [34]. These comparative insights suggest that while physical and hybrid modeling approaches remain indispensable for comprehensive oceanographic forecasting, data-driven methods like CNN (Conv1D) offer scalable and accurate alternatives for specific tasks such as drifting buoy trajectory prediction. The findings of this study contribute to a growing body of evidence supporting the integration of machine learning into marine research, with implications for advancing search and rescue operations, environmental monitoring, and maritime safety. As mentioned, the findings of this study align with and expand upon previous research in time-series prediction and trajectory modeling, as summarized in Table 6.

4. Conclusion

This study evaluates the predictive capabilities of two deep learning models, GRU and CNN (Conv1D), in forecasting the trajectories of drifting buoys.

The focus is on their ability to process time-series and spatial data, both of which are crucial for accurate oceanographic modeling. The experimental results demonstrate that both models, when appropriately configured, exhibit remarkable predictive performance, achieving a near-perfect fit to the input data. This underscores their effectiveness in handling sequential data, making them suitable for marine and oceanographic applications. Among the two architectures, CNN (Conv1D) consistently outperformed GRU across all key performance metrics, including Mean Squared Error (MSE), Root Mean Squared Error (RMSE), and Mean Absolute Error (MAE). A particularly notable finding is that CNN (Conv1D) reduced prediction errors by up to 50% compared to GRU, demonstrating its superior ability to capture complex patterns in buoy movement data.

The study further emphasizes the significance of optimizing model configurations to achieve the best predictive accuracy. Specifically, the results suggest that for different buoy datasets, distinct filter configurations yield optimal performance. For one dataset, the best results were achieved with 256 filters in the hidden layers, while another dataset performed optimally with 128 filters. Moreover, a key observation is that larger datasets significantly enhance model accuracy, highlighting the necessity of sufficient and high-quality data for training deep learning models effectively. These insights reinforce the substantial potential of deep learning in improving the accuracy of trajectory forecasting in marine and oceanographic research. Given CNN (Conv1D)'s superior performance, it presents itself as a robust tool for analyzing similar datasets and tackling challenges in ocean monitoring and forecasting.

Additionally, the study addresses concerns regarding model overfitting by implementing a structured data preprocessing pipeline, including normalization and an appropriate train-test split ratio of 70-30. However, to further enhance model generalizability, future research should focus on validating these models using independent datasets from different time frames and geographic locations. Such an approach will ensure that the models remain robust when applied to real-world data and will mitigate dataset-specific biases. To further strengthen predictive reliability, techniques such as cross-validation and hyperparameter tuning should also be explored. Furthermore, future studies should investigate how combining deep learning models can enhance drifting buoy data analysis.

One limitation of this study is that it relies on specific buoy datasets, which may constrain the generalizability of the findings. To address this, subsequent research should involve model validation across diverse oceanic regions with varying environmental conditions. Additionally, implementing cross-validation strategies can help assess the robustness of the models across different datasets. Another crucial aspect that requires attention in future research is the prediction of buoy positions in independent scenarios, which was not explored in this study. Expanding the research scope to include a broader range of ocean conditions and integrating additional environmental factors, such as satellite data, could further enhance model versatility and reliability. These improvements will contribute to refining deep learning applications for oceanographic studies, maritime navigation, and environmental monitoring.

References

- [1] Ingleby, B. and Isaksen, L., (2018). Drifting Buoy Pressures: Impact on NWP. *Atmospheric Science Letters*, Vol. 19(6). <https://doi.org/10.1002/asl.822>.
- [2] Horányi, A., Cardinali, C. and Centurioni, L., (2017). The Global Numerical Weather Prediction Impact of Mean-sea-level Pressure Observations from Drifting Buoys. *Quarterly Journal of The Royal Meteorological Society*, Vol. 143(703), 974-985. <https://doi.org/10.1002/qj.2981>.
- [3] Chen, W., Sun, Y., Liang, Y., Han, Z. and Su, J., (2019). Study on Buoys for Trajectory Prediction Simulation of Maritime Drifting Objects. *Academic Journal of Engineering Technology Science*, Vol. 2(2), 66-75. <https://doi.org/10.25236/AJETS.020043>.
- [4] Christensen, K. H., Breivik, Ø., Dagestad, K. F., Röhrs, J. and Ward, B., (2018). Short-term Predictions of Oceanic Drift. *Oceanography*, Vol. 31(3), 59-67. <https://www.jstor.org/stable/26509095>.
- [5] Tamtare, T., Dumont, D. and Chavanne, C., (2022). The Stokes Drift in Ocean Surface Drift Prediction. *Journal of Operational Oceanography*, Vol. 15(3), 156-168. <https://doi.org/10.1080/1755876X.2021.1872229>.
- [6] Blockley, E., Martin, M. and Hyder, P., (2012). Validation of FOAM Near-Surface Ocean Current Forecasts Using Lagrangian Drifting Buoys. *Ocean Science*, Vol. 8(4), 551-565. <https://doi.org/10.5194/os-8-551-2012>.

- [7] Vandembulcke, L., Beckers, J. M., Lenartz, F., Barth, A., Poulain, P. M., Aidonidis, M., Meyrat, J., Arduin, F., Tonani, M., Fratianni, C., Torrisi, L., Pallela, D., Pallela, D., Chiggiato, J., Tudor, M., Book, J. W., Martin, P., Peggion, G. and Rixen, M., (2009). Superensemble Techniques: Application to Surface Drift Prediction. *Progress in Oceanography*, Vol. 82(3), 149-167. <https://doi.org/10.1016/j.pocean.2009.06.002>.
- [8] Botvynko, D., Granero-Belinchon, C., Gennip, S. V., Benzinou, A. and Fablet, R., (2023). Deep Learning for Lagrangian Drift Simulation at the Sea Surface. In *ICASSP 2023-2023 IEEE International Conference on Acoustics, Speech and Signal Processing (ICASSP)*. IEEE. <https://doi.org/10.1109/ICASSP49357.2023.10094622>.
- [9] Pärt, S., Björkqvist, J. V., Alari, V., Maljutenko, I. and Uiboupin, R., (2023). An Ocean-Wave-Trajectory Forecasting System for the Eastern Baltic Sea: Validation Against Drifting Buoys and Implementation for Oil Spill Modeling. *Marine Pollution Bulletin*, Vol. 195, 115497. <https://doi.org/10.1016/j.marpolbul.2023.115497>.
- [10] Aksamit, N. O., Sapsis, T. P. and Haller, G., (2019). Machine-learning Ocean Dynamics from Lagrangian Drifter Trajectories. *arXiv preprint arXiv*. <https://doi.org/10.48550/arXiv.1909.12895>.
- [11] Baidai, Y., Dagorn, L., Amande, M. J., Gaertner, D. and Capello, M., (2020). Machine Learning for Characterizing Tropical Tuna Aggregations under Drifting Fish Aggregating Devices (DFADs) from Commercial Echosounder Buoys Data. *Fisheries Research*, Vol. 229. <https://doi.org/10.1016/j.fishres.2020.105613>.
- [12] Diamant, R., (2020). Prediction of Water Current Using a Swarm of Submerged Drifters. *IEEE Sensors Journal*, Vol. 20(19), 11598-11607. <https://doi.org/10.1109/JSEN.2020.2996299>.
- [13] Apel, H., Hung, N. G., Thoss, H. and Schone, T., (2012). GPS Buoys for Stage Monitoring of Large Rivers. *Journal of Hydrology*, Vol. 412, 182-192. <https://doi.org/10.1016/j.jhydrol.2011.07.043>.
- [14] Häfner, D., Gemmrich, J. and Jochum, M., (2021). FOWD: A Free Ocean Wave Dataset for Data Mining and Machine Learning. *Journal of Atmospheric Oceanic Technology*, Vol. 38(7), 1305-1322. <https://doi.org/10.1175/JTECH-D-20-0185.1>.
- [15] Pokhrel, P., (2021). Machine Learning in Weakly Nonlinear Systems: A Case Study on Significant Wave Heights. *arXiv preprint arXiv*. <https://doi.org/10.48550/arXiv.2105.08583>.
- [16] Mozo, A., Morón-López, C. J., Vakaruk, S., Pompa-Pernía, A. G., González-Prieto, A., Aguilar, J. A. P., Gómez-Canaval, S. and Ortiz, J. M., (2022). Chlorophyll Soft-sensor Based on Machine Learning Models for Algal Bloom Predictions. *Scientific Reports*, Vol. 12(1). <https://doi.org/10.1038/s41598-022-17299-5>.
- [17] Bhaganagar, K., Kolar, P., Faruqui, S. H. A., Bhattacharjee, D., Alaeddini, A. and Subbarao, K., (2022). A Novel Machine-Learning Framework with a Moving Platform for Maritime Drift Calculations. *Frontiers in Marine Science*, Vol. 9. <https://doi.org/10.3389/fmars.2022.831501>.
- [18] Song, M., Hu, W., Liu, S., Chen, S., Fu, X., Zhang, J., Li, W. and Xu, Y., (2024). Developing an Artificial Intelligence-Based Method for Predicting the Trajectory of Surface Drifting Buoys Using a Hybrid Multi-Layer Neural Network Model. *Journal of Marine Science Engineering*, Vol. 12(6). <https://doi.org/10.3390/jmse12060958>.
- [19] Hackett, B., Breivik, Ø. and Wettre, C., (2006). Forecasting The Drift of Objects and Substances in the Ocean. *Ocean Weather Forecasting: An Integrated View of Oceanography*, 507-523. https://doi.org/10.1007/1-4020-4028-8_23.
- [20] Kim, J. C., Dae, H., Sim, J. E., Son, Y. T., Bang, K. Y. and Shin, S., (2023). Validation of Opendrift-based Drifter Trajectory Prediction Technique for Maritime Search and Rescue. *Journal of Ocean Engineering Technology*, Vol. 37(4), 145-157. <https://doi.org/10.26748/KSOE.2023.018>.
- [21] Trong, N. G., Quang, P. N., Cuong, N. V., Le, H. A., Nguyen, H. L. and Tien Bui, D., (2023). Spatial Prediction of Fluvial Flood in High-Frequency Tropical Cyclone Area Using TensorFlow 1D-convolution Neural Networks and Geospatial Data. *Remote Sensing*, Vol. 15(22). <https://doi.org/10.3390/rs15225429>.
- [22] Trong, N. G., Thanh, P. T., Tinh, L. D., Thao, N. B. and Elshewy, M. A., (2025). Application of Deep Learning Models for Groundwater Data Analysis: A Comparative Study of CNN (Conv1D), SimpleRNN, and Gated Recurrent Unit (GRU) Models. *International Journal of Geoinformatics*, Vol. 21(3), 100-114. <https://doi.org/10.52939/ijg.v21i3.4001>.

- [23] Shi, H., Pan, C., Yang, L. and Gu, X., (2021). AGG: A Novel Intelligent Network Traffic Prediction Method Based on Joint Attention and GCN-GRU. *Security Communication Networks*, Vol. 2021(1). <https://doi.org/10.1155/2021/7751484>.
- [24] Yu, F. and Koltun, V., (2015). Multi-scale Context Aggregation by Dilated Convolutions. *arXiv Preprint arXiv*. <https://doi.org/10.48550/arXiv.1511.07122>.
- [25] Shi, X., Chen, Z., Wang, H., Yeung, D. Y., Wong, W. K. and Woo, W. C., (2015). Convolutional LSTM Network: A Machine Learning Approach for Precipitation Nowcasting. *Advances in Neural Information Processing Systems*, 1-9. <https://doi.org/10.48550/arXiv.1506.04214>.
- [26] Platform Drifting Buoy. NASA/CASEI. [online]. Available: <https://impact.earthdata.nasa.gov/casei/platform/Drifting%20Buoy/>. [Accessed Oct. 2, 2024].
- [27] Vietnam Ministry of Natural Resources and Environment (2020). Scenario of Climate Change, Sea Level Rise for Vietnam in 2020, *Technical Report*, Hanoi. <https://pilot.dcc.gov.vn/en/publications/scenario-of-climate-change-sea-level-1508>.
- [28] Tinh, L. Đ., Thao, D. T. P., Thang, T. D., Hop, D. T. and Trong, N. G., (2024). Evaluating the Performance of CNN (Conv1D) and CNN (Conv3D) Models in GNSS Data Analysis. *Journal of Hydrometeorology*, Vol. 771, 55-64. [https://doi.org/10.36335/VNJHM.2025\(771\).55-64](https://doi.org/10.36335/VNJHM.2025(771).55-64).
- [29] Tinh, L. D., Quoc, H. N. D. and Trong, N. G., (2024). Exploring the Training Results of Machine Learning Models Using Different Batch Sizes and Epochs: A Case Study with GNSS Time Series Data. *Journal of Hydrometeorology*, Vol. 19, 90-99. [https://doi.org/10.36335/VNJHM.2024\(19\)](https://doi.org/10.36335/VNJHM.2024(19)).
- [30] Trọng, N. G. and Quý, B. N., (2024). Analyzing Tidal Data Sequences Using Gated Recurrent Unit (GRU). *Journal of Hydrometeorology*, Vol. 765, 39-46. [https://doi.org/10.36335/VNJHM.2024\(765\)](https://doi.org/10.36335/VNJHM.2024(765)).
- [31] Campesato, O., (2020). *Python 3 for Machine Learning*. Mercury Learning and Information. Dulles, VA 20166.
- [32] Raschka, S. and Mirjalili, V., (2019). *Python Machine Learning: Machine Learning and Deep Learning with Python, Scikit-learn, and TensorFlow 2* (Third Edition). Packt Publishing Ltd. Birmingham - Mumbai.
- [33] Alpaydin, E., (2020). *Introduction to Machine Learning (Fourth Edition)*. MIT Press. Cambridge, Massachusetts, London, England.
- [34] Kiranyaz, S., Avci, O., Abdeljaber, O., Ince, T., Gabbouj, M. and Inman, D. J., (2021). 1D Convolutional Neural Networks and Applications: A Survey. *Mechanical Systems Signal Processing*, Vol. 151. <https://doi.org/10.1016/j.ymssp.2020.107398>.
- [35] Cho, K., Van Merriënboer, B., Gulcehre, C., Bahdanau, D., Bougares, F., Schwenk, H. and Bengio, Y. (2014). Learning Phrase Representations Using RNN Encoder-decoder for Statistical Machine Translation. *arXiv preprint arXiv*. <https://doi.org/10.48550/arXiv.1406.1078>.
- [36] Hai, P., Minh, T., Luận, V., and Trung, T. (2023). Machine Learning Models for Fine Particulate Matter (PM2.5) Prediction: A Case Study in Bac Ninh Province, Vietnam. *International Journal of Geoinformatics*, Vol. 19(12), 30–50. <https://doi.org/10.52939/ijg.v19i12.2975>.
- [37] Willmott, C. J. and Matsuura, K., (2005). Advantages of the Mean Absolute Error (MAE) Over the Root Mean Square Error (RMSE) in Assessing Average Model Performance. *Climate Research*, Vol. 30(1), 79-82. <https://doi.org/10.3354/cr030079>.
- [38] Nagelkerke, N. J., (1991). A Note on a General Definition of the Coefficient of Determination. *Biometrika*, Vol. 78(3), 691-692.